Single Molecule Spectroscopy of Organic Dye Nanoparticles

ARTICLE *in* NANO LETTERS · AUGUST 2005

Impact Factor: 13.59 · DOI: 10.1021/nl050567j · Source: PubMed

NANO LETTERS

2005
Vol. 5, No. 7
1321−1325

Single Molecule Spectroscopy of Organic Dye Nanoparticles

Andre J. Gesquiere,[†] Takayuki Uwada,[‡] Tsuyoshi Asahi,[‡] Hiroshi Masuhara,[‡] and Paul F. Barbara*,[†]

Center for Nano- and Molecular Science and Technology, Department of Chemistry and Biochemistry, University of Texas at Austin, Austin, Texas 78712, and Department of Applied Physics and Handai Frontier Research Center, Osaka University, Suita, Osaka 565-0871, Japan

Received March 23, 2005

ABSTRACT

Organic dye nanoparticles 1–13 nm in height and 10–45 nm in width were prepared by the reprecipitation method. With single-molecule/nanoparticle spectroscopy, two distinct types of nanoparticles were found: particles with blue emission and particles with red emission. The difference in spectral characteristics is attributed to the presence of two morphological types of particles in the samples. The presence of two types of nanoparticles in the samples was further corroborated by our ability to separate blue nanoparticles from red nanoparticles by centrifugation.

Organic fluorescent semiconductor materials are found in many promising device applications (e.g., organic light-emitting diodes[1,2]). Materials for these applications range from small-molecule aromatics, such as the widely utilized perylene-diimides, to large-molecular-weight conjugated polymers.[3−7] An active area of research for organic semiconductors is the study of how the complex, nanostructured morphology of these materials affects their fluorescence properties.[8] For example, the nanostructure of organic thin films has been extensively investigated by near-field scanning optical microscopy (NSOM) revealing strong correlations among the morphology, fluorescence yields, and spectra.[4,8−10] Unfortunately, the limited spatial resolution of NSOM for these applications and the complex 3D structure of the thin films has precluded the investigation of single morphological domains, which would offer the most useful information.

An alternative approach—single-particle spectroscopy (generally designated by the term single molecule spectroscopy − SMS)—has led to unprecedented data on the nature of optical excitations and other aspects of the spectroscopy, photophysics, and photochemistry of organics in the single morphological domain.[11−14] To date, SMS has been applied to isolated single polymer chains (molecules) of conjugated polymers.[15−20] In the present letter, we extend this work for the first time to nanoparticles that consist of a few thousand organic molecules, representing a multichromophoric system. Organic nanoparticles are of interest because they represent an intermediate situation between single molecules and bulk materials, representing a multichromophoric system.

The most popular methods for organic nanoparticle fabrication are laser ablation,[21] the sol−gel method,[22] and reprecipitation,[23] the latter of which is being used in this letter. The fabrication of these particles is currently not well controlled, leading to broad size distributions in the organic nanoparticle samples (in stark contrast to the well-controlled size distributions obtained for semiconductor nanoparticles). Because it has been suggested in the literature that organic nanoparticles can show size-dependent optical properties, it is useful to investigate individual nanoparticles one at a time.[24−26] Single-molecule/nanoparticle spectroscopy is the ideal tool to use to address this issue.

In this letter, we report the characterization of *N*,*N*′-bis(2,5-di-*tert*-butylphenyl)-3,4,9,10-perylenedicarboximide (DBPI, see **1** with R = *tert*-butyl) nanoparticles by atomic force microscopy (AFM), bulk spectroscopy, and single-molecule/particle spectroscopy. Single molecule spectroscopy (SMS) allows complex and heterogeneous systems to be studied in detail compared to bulk studies.[11−14] This technique has been previously used to study the photophysics of multichromophoric systems including conjugated polymers such as MEH−PPV and dye-substituted dendrimers.[15−19,27] These multichromophoric systems have been shown to have coupled chromophores, leading to phenomena such as fluorescence blinking and energy funneling. A significant fraction of the nanoparticles (25%) exhibited fluorescence intermittence (i.e., "blinking"). Blinking in a multichromo-

* To whom correspondence should be addressed. E-mail: p.barbara@mail.utexas.edu.
[†] University of Texas at Austin.
[‡] Osaka University.

10.1021/nl050567j CCC: $30.25
Published on Web 05/25/2005

phoric system is evidence of efficient interchromorphore coupling and energy transfer. It has been extensively observed for conjugated polymer molecules that possess hundreds of covalently linked chromophores. The present letter is the first report of blinking in multichromophoric nanoparticles of DBPI dye molecules.

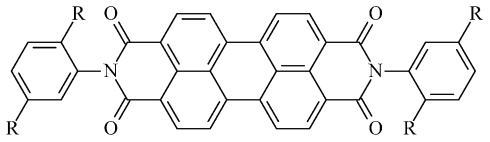

1

Furthermore, a key result is that the bulk emission spectra of DBPI nanoparticles in solution, which show both monomer-like and excimer-like emission of DBPI, can in fact be explained by the presence of two morphological types of nanoparticles with distinctively different spectral characteristics, as shown by single-particle spectroscopy. These particles could in fact be separated by centrifugation.

DBPI (Aldrich) nanoparticles were prepared according to the reprecipitation method.[23] A volume of 100 μL of a 1 mM DBPI solution in 1-methyl-2-pyrrolidinone (NMP, Aldrich) was injected into 10 mL of stirred water. NMP is a good solvent for DBPI and mixes well with water, which is a nonsolvent for DBPI. A clear, pink solution was obtained, which was used as a mother solution of DBPI nanoparticles. A Digital Instruments (Veeco) Dimension 3100 AFM system was used for tapping-mode imaging of the DBPI nanoparticles. A drop of the nanoparticle solution in water was cast on freshly cleaved mica and allowed to dry in vacuum before imaging. Absorption spectra were acquired with an Agilent 8453 UV/Vis spectrophotometer. Fluorescence spectra were acquired by excitation at 490 nm with a SPEX Fluorolog 3. The confocal microscope has been described previously.[28] Films of nanoparticles in poly(vinyl alcohol) (PVA) were spin coated onto glass and sealed with a 100 nm gold film to keep oxygen from penetrating the sample. Individual nanoparticles were irradiated by the 488 or 514.5 nm lines of an argon ion laser. The laser intensity at the sample was 450 W/cm^2. The centrifuged samples were prepared as follows. Nanoparticles in water were deposited on top of a sucrose density gradient ranging from 10 to 30% density and subjected to centrifugation for 18 h at 29 000 rpm in a Beckman SW41 rotor at 4 °C and a 10^{-4} Torr atmosphere. A pink band at around 20% sucrose density was visible with the naked eye after centrifugation. The centrifuged solution was fractioned into 420 μL aliquots, and some of these fractions were chosen for spectroscopic investigation (e.g., Figure 3B−D).

The absorption spectrum of DBPI dissolved in NMP is shown in Figure 1A. The absorption maximum is located at 526 nm (0−0 vibronic peak). The absorption peak at 490 nm corresponds to the 0−1 vibronic peak.[29] Emission spectra of DBPI dissolved in NMP were also collected; see Figure 1A. The emission maximum is located at 536 nm (0−0 vibronic peak), and the emission peak at 578 nm corresponds to the 1−0 vibronic peak.[29]

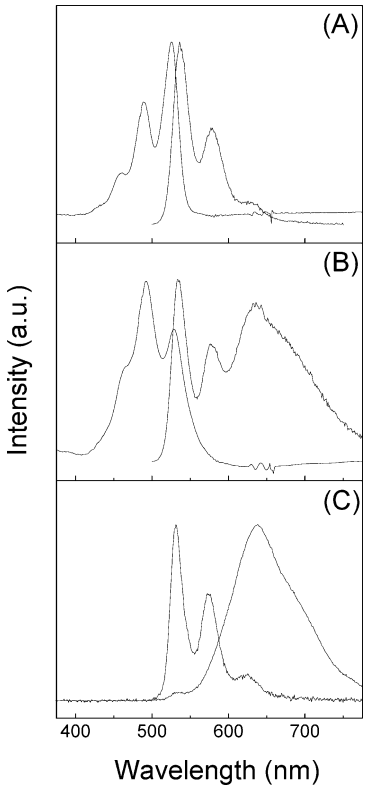

Figure 1. (A) Absorption and emission spectra of DBPI dissolved in NMP. (B) Absorption and emission spectra of DBPI nanoparticles dispersed in a PVA/water solution. (C) Sub-ensembles of single-nanoparticle spectra. These were collected for single DBPI nanoparticles dispersed in a PVA matrix.

Nanoparticles were prepared by the reprecipitation method.[23] Before spinning onto a glass substrate, the nanoparticle solution was added to PVA solutions of 2 or 4% in water, resulting in film thicknesses of 40 and 80 nm, respectively. The absorption spectrum of the nanoparticle solution in PVA is shown in Figure 1B. The nanoparticle absorption spectra are similar to the absorption spectra of DBPI molecularly dissolved in NMP (Figure 1A, B). However, the intensity of the 0−1 vibronic peak has surpassed that of the 0−0 vibronic peak. The emission spectra of the nanoparticles show a mixture of monomer-like (blue) and excimer-like (red) emission. The blue emission peaks (533, 578 nm) coincide with the 0−0 and 1−0 vibronic peaks in the emission spectra observed for DBPI dissolved in NMP (i.e., monomer-like emission). The red emission band at 637 nm is consistent with observations made for DBPI in bulk solids and is assigned to emission from a self-trapped exciton state (i.e., excimer emission (dimer of molecules in the crystal)).[29] It is known that PVA influences the bulk spectroscopy of perylene nanocrystals and that the blue emission is enhanced when PVA is present.[30] This was also observed for the DBPI nanoparticles. With single-particle spectroscopy, we were able to uncover the underlying reason for these observations (see below).

The nanoparticle size and shape were characterized by tapping-mode atomic force microscopy (AFM). An AFM image of nanoparticles on mica is shown in Figure 2. A particle analysis done on AFM images of hundreds of

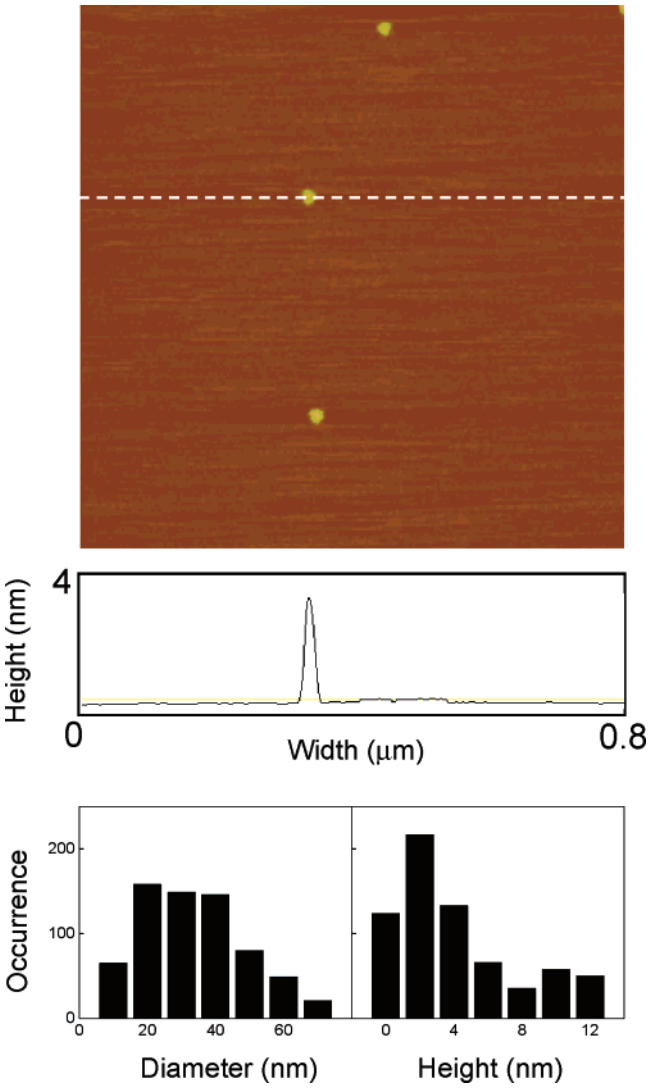

Figure 2. (Top) AFM image of DBPI nanoparticles deposited on mica. A line scan is shown for one of the particles (- - -). (Bottom) Histogram of the height and width determined for 680 particles.

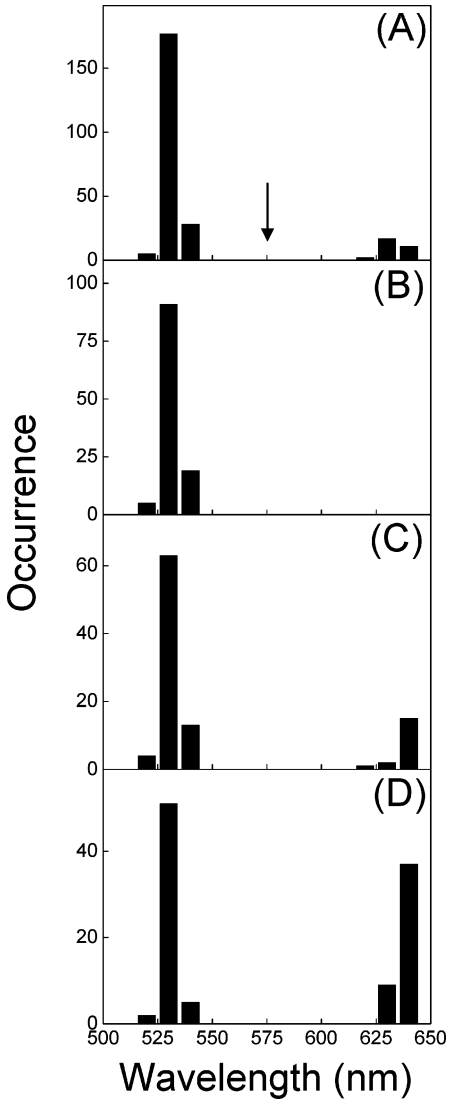

Figure 3. Histograms of emission maxima of single-nanoparticle spectra. (A) Histogram of the emission maxima for individual particles in the ensemble. The arrow indicates the wavelength that was chosen to distinguish between the red and blue sub-ensembles. (B−D) Data for samples that were prepared by centrifugation in a sucrose gradient. (B) Sucrose density, 7%. Only blue particles are present in this fraction. (C) Sucrose density, 15%. (D) Sucrose density, 20%. In the histograms in panels C and D, a mixture of red and blue particles is evident, with a larger fraction of red nanoparticles in the sample that was extracted at 20% sucrose density.

nanoparticles reveals a broad size distribution. The height of the nanoparticles in AFM images (e.g., Figure 2) varied from 1 to 13 nm, and the apparent width varied from 20 to 65 nm. Because the particle shape is clearly platelike, the width can be deconvoluted as follows

$$D = 2\sqrt{2Rh - h^2} \qquad (1)$$

where D is the error in the lateral dimensions of the nanoparticle introduced by the convolution of tip and nanoparticle, R is the tip radius, and h is the height of the platelike particle.[31] The deconvoluted width of the particles ranges from 10 to 45 nm.

Fluorescence spectra and fluorescence time trajectories were collected for 230 individual DBPI nanoparticles. Each DBPI nanoparticle has either a blue or red emission maximum. Figure 1C shows "sub-ensemble" spectra, constructed by averaging the spectra of individual nanoparticles, after sorting the spectra into red and blue spectra by using the emission maxima as a sorting criterion. Figure 3A shows a histogram of the emission maxima for individual particles, with an arrow located at the wavelength that was chosen to distinguish between the red and blue sub-ensembles.

The blue-emitting DBPI nanoparticles have an emission that closely resembles the spectrum of DBPI in the good solvent, NMP (Figure 1A). The red-emitting nanoparticles have a spectrum that resembles that previously observed for the excimer emission of powders and films of DBPI.[29] On the basis of the presence of exclusively red-emitting or exclusively blue-emitting nanoparticles in the thin film samples, we conclude that the dual emission band in Figure 1B for the PVA/water solutions (from which the nanopar-

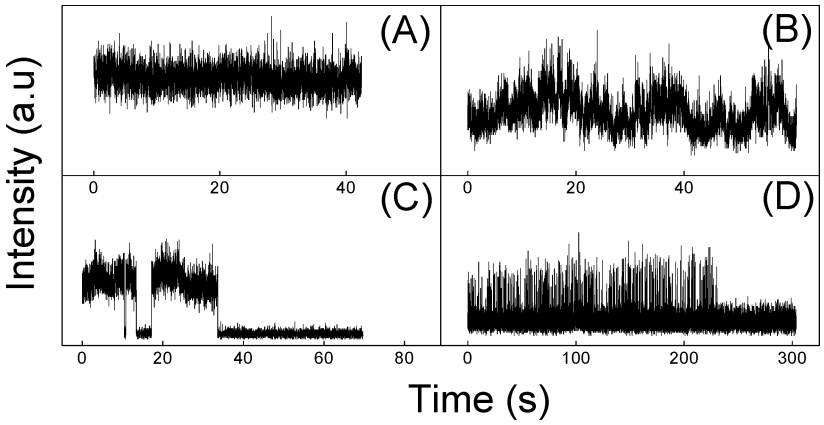

Figure 4. (A−C) Fluorescence intensity−time transients of DBPI nanoparticles. The nanoparticles have (A) a constant intensity or (B) a fluctuating intensity or show (C) fluorescence intensity blinking. (D) Fluorescence intensity−time transients of DBPI single molecules. Intensity bursts are observed.

ticles are derived) is due to the sum of spectra from two distinct types of particles.

All nanoparticle samples prepared by the described procedures were mixtures of blue and red particles. However, we successfully separated blue nanoparticles from red nanoparticles via centrifugation. Figure 3B−D shows histograms of emission maxima for three different samples. These samples represent different fractions taken from the centrifuged solution. The fraction collected at 7% sucrose density contains only blue particles (Figure 3B). At 15% sucrose density, blue and red particles are present in a ratio of ∼8:1 (Figure 3C). For fractions around 20% sucrose density, we found a mixture of blue and red particles that are present in a ratio of ∼1:1 (Figure 3D). For fractions higher than 25% sucrose density, we did not find a significant presence of either blue or red particles. The density and size of the red particles is such that the centrifugation process can remove red particles from the fractions with lower sucrose gradients, leaving only blue particles. However, we could not obtain a fraction that contained only red particles.

The two types of particles in the samples probably possess different crystal morphologies. Perylene is in fact known to occur in two crystal morphologies: the α and β forms.[32,33] α-Perylene has a dimeric crystal structure in which pairs of molecules are oriented face-to-face, whereas β-perylene has a monomeric crystal structure. The α and β crystals have different emission spectra in which α crystals show a broad structureless red emission (self-trapped exciton, i.e., excimer) and β crystals show blue emission with a vibrational series that can be assigned to a self-trapped exciton state related to a crystal structure in which molecules are not packed face-to-face (i.e., monomer-like emission).[32,33] Alternatively, the morphological difference could find its origin in the size of the nanoparticles, where small amorphous particles could show blue emission and larger crystalline particles could show red emission. The difference in particle size is also discussed in view of observed fluorescence intensity fluctuations (see below). Furthermore, DBPI is sterically hindered and might not be readily packed into a face-to-face fashion, as one would typically expect for perylene-type molecules. An X-type packing structure was previously proposed for DBPI by analogy to *N*,*N*′-bis(2,6-xylyl)-3,4,9,10-perylenedicarboximide. The latter molecule indeed shows monomer-like characteristics in the absorption spectra of its films.[34]

Three types of fluorescence time trajectories were found for the nanoparticles: trajectories with constant intensity, trajectories with intensity fluctuations, and trajectories that show blinking. These are shown in Figure 4A−C. Time transients of red particles show only constant intensity or intensity fluctuations. Blue particles, however, show all three types of behavior.

The fluorescence intensity blinking observed for blue particles is reminiscent of that observed in the multichromophoric conjugated polymer MEH−PPV. Blinking of the MEH−PPV fluorescence intensity has been shown to be caused by reversible oxidation/reduction events at special sites in the polymer backbone to which the excitation energy is efficiently funneled.[15−17] Furthermore, MEH−PPV molecules can exhibit either blue or red emission. The special sites are lower-energy chromophores that are formed by intramolecular chain−chain contacts, and these emissive low-energy chromophores exhibit red emission. DBPI nanoparticles could develop low-energy trap sites. In fact, this has been shown in multichromophoric perylene-substituted dendrimers with eight chromophores, which also exhibit fluorescence blinking.[27] Intensity fluctuations, however, are a typical observation for multichromophoric systems in which the chromophores are not coupled, as mainly observed for the DBPI nanoparticles. Either the nanoparticles do not commonly develop the aforementioned low-energy trap sites or the size of the nanoparticles is so large that energy funneling is inefficient for the majority of the chromophores in the nanoparticles.

Considering the fact that red nanoparticles have a higher fluorescence intensity in the time transients and spectra than blue nanoparticles, the red nanoparticles can be assumed to be larger than the blue nanoparticles. Indirect evidence to support this suggestion is the observation that using a higher dye concentration in the synthesis procedure produces samples with more red particles, and these samples were found on average to have a larger particle size (determined by AFM).

As a control experiment, single DBPI molecules were dispersed in a PMMA matrix on glass and sealed with a Au film. Time transients collected for these oxygen-depleted single dye samples show a telegraphic fluorescence signal (intensity bursts, Figure 4D). This observation was previously made for the single chromophoric molecule DiI and is caused by triplet bottlenecking.[28,35] In fact, these molecules are very dim in the confocal fluorescence images. Thus, single dye impurities in the samples are easily distinguished from DBPI nanoparticles.

Previous studies have shown that perylene and its derivatives exhibit dual emission bands in environments that favor aggregation.[25,30] The dual emission was attributed to either dual-emitting nanoparticles with both monomer-like and excimer-like bands (due to a rearrangement of dye molecules at the surface of the nanoparticles)[30] or a size effect for large nanoparticles where dual-emitting particles are large particles that have domains of different morphologies.[25] The latter observation was also made for the platelike crystals formed by the dye 1,1′-diethyl-2,2′-cyanine iodide (PIC), in which red-shifted emission was shown to be related to defects in the crystal structure at the interface between crystal plates.[36] Interestingly, different from the observations made for PIC crystals and nanocrystals fabricated from unfunctionalized perylene, DBPI nanoparticles show dual emission that is due to the presence of two distinct types of particles with different morphologies and, as a result, different spectral characteristics.

In conclusion, disklike dye nanoparticles 1−13 nm in height and 10−45 nm in width were prepared by the reprecipitation method. These dye nanoparticles were studied in PVA/water solution by bulk spectroscopy and in a PVA matrix by single-particle spectroscopy. The bulk emission spectrum has the characteristics of both monomer-like and excimer-like emission. By virtue of single-particle spectroscopy, we were able to correlate this observation with the presence of two distinct types of nanoparticles in the samples: nanoparticles with blue emission and nanoparticles with red emission. This finding was further corroborated by the ability to separate blue particles from red particles by centrifugation.

Acknowledgment. We thank Dr. Scott Stevens of the Institute for Cellular and Molecular Biology at the University of Texas at Austin for indispensable assistance with the centrifugation experiments and discussions. We gratefully acknowledge the National Science Foundation, the Robert A. Welch Foundation, the UOMOTO Foundation, and MEXT for supporting this research.

References

(1) Tang, C. W.; Vanslyke, S. A. *Appl. Phys. Lett.* **1987**, *51*, 913.
(2) Friend, R. H.; Gymer, R. W.; Holmes, A. B.; Burroughes, J. H.; Marks, R. N.; Taliani, C.; Bradley, D. D. C.; Dos Santos, D. A.; Bredas, J. L.; Logdlund, M.; Salaneck, W. R. *Nature* **1999**, *397*, 121.
(3) Shirota, Y. *J. Mater. Chem.* **2005**, *15*, 75.
(4) Adams, D. M.; Kerimo, J.; O'Connor, D. B.; Barbara, P. F. *J. Phys. Chem. A* **1999**, *103*, 10138.
(5) Kim, J. Y.; Bard, A. J. *Chem. Phys. Lett.* **2004**, *383*, 11.
(6) Bernius, M. T.; Inbasekaran, M.; O'Brien, J.; Wu, W. S. *Adv. Mater.* **2000**, *12*, 1737.
(7) Heeger, A. J. *Angew. Chem., Int. Ed.* **2001**, *40*, 2591.
(8) Schwartz, B. J. *Annu. Rev. Phys. Chem.* **2003**, *54*, 141.
(9) Vanden Bout, D. A.; Kerimo, J.; Higgins, D. A.; Barbara, P. F. *Acc. Chem. Res.* **1997**, *30*, 204.
(10) McNeill, J. D.; O'Connor, D. B.; Barbara, P. F. *J. Chem. Phys.* **2000**, *112*, 7811.
(11) Nie, S.; Zare, R. *Annu. Rev. Biophys. Biomol. Struct.* **1997**, *26*, 567.
(12) Xie, X. S.; Trautman, J. K. *Annu. Rev. Phys. Chem.* **1998**, *49*, 441.
(13) Moerner, W. E.; Orrit, M. *Science* **1999**, *283*, 1670.
(14) Kulzer, F.; Orrit, M. *Annu. Rev. Phys. Chem.* **2004**, *55*, 585.
(15) Vandenbout, D. A.; Yip, W. T.; Hu, D. H.; Fu, D. K.; Swager, T. M.; Barbara, P. F. *Science* **1997**, *277*, 1074.
(16) Hu, D. H.; Yu, J.; Wong, K.; Bagchi, B.; Rossky, P. J.; Barbara, P. F. *Nature* **2000**, *405*, 1030.
(17) Yu, J.; Hu, D. H.; Barbara, P. F. *Science* **2000**, *289*, 1327.
(18) Huser, T.; Yan, M.; Rothberg, L. J. *Proc. Natl. Acad. Sci. U.S.A.* **2000**, *97*, 11187.
(19) Schindler, F.; Lupton, J. M.; Feldmann, J.; Scherf, U. *Proc. Natl. Acad. Sci. U.S.A.* **2004**, *101*, 14695.
(20) Ronne, C.; Tragardh, J.; Hessman, D.; Sundstrom, V. *Chem. Phys. Lett.* **2004**, *388*, 40.
(21) Sugiyama, T.; Asahi, T.; Masuhara, H. *Chem. Lett.* **2004**, *33*, 724.
(22) Ibanez, A.; Maximov, S.; Guin, A.; Chaillout, C.; Baldeck, P. L. *Adv. Mater.* **1998**, *10*, 1540.
(23) Kasai, H.; Nalwa, H. S.; Oikawa, H.; Okada, S.; Matsuda, H.; Minami, N.; Kakuta, A.; Ono, K.; Mukoh, A.; Nakanishi, H. *Jpn. J. Appl. Phys., Part 2* **1992**, *31*, L1132.
(24) Xie, R. M.; Fu, H. B.; Ji, X. H.; Yao, J. N. *J. Photochem. Photobiol., A* **2002**, *147*, 31.
(25) Kasai, H.; Kamatani, H.; Yoshikawa, Y.; Okada, S.; Oikawa, H.; Watanabe, A.; Itoh, O.; Nakanishi, H. *Chem. Lett.* **1997**, 1181.
(26) Kurokawa, N.; Yoshikawa, H.; Hirota, N.; Hyodo, K.; Masuhara, H. *ChemPhysChem* **2004**, *5*, 1609.
(27) Hofkens, J.; Maus, M.; Gensch, T.; Vosch, T.; Cotlet, M.; Kohn, F.; Herrmann, A.; Mullen, K.; De Schryver, F. *J. Am. Chem. Soc.* **2000**, *122*, 9278.
(28) Yip, W. T.; Hu, D. H.; Yu, J.; Vanden Bout, D. A.; Barbara, P. F. *J. Phys. Chem. A* **1998**, *102*, 7564.
(29) Ford, W. E.; Kamat, P. V. *J. Phys. Chem.* **1987**, *91*, 6373.
(30) Xie, R. M.; Xiao, D. B.; Fu, H. B.; Ji, X. H.; Yang, W. S.; Yao, J. N. *New J. Chem.* **2001**, *25*, 1362.
(31) Plaschke, M.; Schafer, T.; Bundschuh, T.; Manh, T. N.; Knopp, R.; Geckeis, H.; Kim, J. I. *Anal. Chem.* **2001**, *73*, 4338.
(32) Tanaka, J. *Bull. Chem. Soc. Jpn.* **1963**, *36*, 1237.
(33) Nishimura, H.; Yamaoka, T.; Mizuno, K.; Iemura, M.; Matsui, A. *J. Phys. Soc. Jpn.* **1984**, *53*, 3999.
(34) Graser, F.; Hadicke, E. *Liebigs Ann. Chem.* **1980**, 1994.
(35) Weston, K. D.; Carson, P. J.; DeAro, J. A.; Buratto, S. K. *Chem. Phys. Lett.* **1999**, *308*, 58.
(36) VandenBout, D. A.; Kerimo, J.; Higgins, D. A.; Barbara, P. F. *J. Phys. Chem.* **1996**, *100*, 11843.

NL050567J